SAND2021-14809C

Sizing Energy Storage to Aid Wind Power Generation: Inertial Support and Variability Mitigation

Atri Bera, Tu Nguyen, Babu Chalamala, and Joydeep Mitra*
Sandia National Laboratories, Albuquerque, NM, USA
{beraatri, tunguy, bchalam}@sandia.gov
*Department of Electrical & Computer Engineering
Michigan State University, East Lansing, MI, USA
mitraj@msu.edu

***Abstract*—Variable energy resources (VERs) like wind and solar are the future of electricity generation as we gradually phase out fossil fuel due to environmental concerns. Nations across the globe are also making significant strides in integrating VERs into their power grids as we strive toward a greener future. However, integration of VERs leads to several challenges due to their variable nature and low inertia characteristics. In this paper, we discuss the hurdles faced by the power grid due to high penetration of wind power generation and how energy storage system (ESSs) can be used at the grid-level to overcome these hurdles. We propose a new planning strategy using which ESSs can be sized appropriately to provide inertial support as well as aid in variability mitigation, thus minimizing load curtailment. A probabilistic framework is developed for this purpose, which takes into consideration the outage of generators and the replacement of conventional units with wind farms. Wind speed is modeled using an autoregressive moving average technique. The efficacy of the proposed methodology is demonstrated on the WSCC 9-bus test system.**

***Index Terms*—energy storage, frequency stability, inertial support, variability mitigation, wind power generation**

I. Introduction

The penetration of wind energy into the power grid is ever-increasing, with the U.S. adding a record 14.2 GW of wind turbine capacity in 2020 [1] alone, despite the ongoing pandemic. Replacing fossil fuel powered electricity generation by wind energy is also crucial for achieving the goals set by the Paris Climate Accords, and this entails increasing the global cumulative installed capacity of onshore wind power to about 1800 GW by 2030 and 5000 GW by 2050 [2]. However, integrating this massive amount of wind energy into the power grid might lead to stability and reliability issues due to the low inertia and intermittent characteristics of wind.

The extensive replacement of conventional synchronous generators with wind farms is decreasing the overall system inertia and thus degrading the frequency response of the system [3]. In addition, the variable and intermittent nature of wind power also negatively affects the reliability of the system, thus leading to greater load curtailment [4]. Energy storage systems (ESS) can provide effective solutions to the aforementioned problems. These devices are well suited for providing multiple services to the power grid due to their flexibility in operation, high ramp rates, and decreasing costs [5]. Studies in the past have proposed approaches to utilize ESS to solve this problems individually. Hu *et al.* in [6] explicitly showed how installation of ESS mitigates the variability of wind power and improves system reliability by performing reliability evaluation of a wind integrated system. Mitra [7] developed a probabilistic method for determining the size of an ESS to achieve a pre-specified reliability target. The sizing of ESSs for providing virtual inertia has been studied in [8]–[10]. Reference [8] proposes a sizing methodology by considering the contribution of the ESS in terms of inertial constant and droop, while [9] proposes an optimal planning strategy for ESS providing inertial support to the grid by utilizing the rate of change of frequency and frequency nadir of the system.

This work adds to the prior art by proposing a planning strategy for sizing ESS to provide inertial support as well as aid in variability mitigation of wind-integrated systems. These are the two most common hurdles faced while integrating wind resources to the power grid and the existing literature do not address these issues jointly. In this work, a probabilistic framework is developed for sizing ESS to assist the wind-integrated system in solving these problems. The quantity of storage required for variability mitigation of wind power is determined by setting a reliability target and minimizing the load curtailment. A Monte Carlo simulation (MCS) technique is used for this purpose. The same algorithm also produces an estimate of the system inertia at each time period, considering the outage of power system equipment and replacement of conventional generation with wind. This estimate of system inertia helps in determining the storage quantity required for inertial support. A few case studies are performed to demonstrate the efficacy of the proposed methodology.

The rest of the the paper is organized as follows. Section II describes the approach used for sizing the ESS for variability mitigation of wind and minimizing the load curtailment. Section III discusses the methods used for estimating system inertia and hence determining the size of ESS required for inertial support. Section IV summarizes wind farm modeling while Section V demonstrates some case studies and presents their results. Section VI provides some concluding remarks.

II. Sizing for Variability Mitigation

First, sizing of the ESS for variability mitigation is discussed. Integration of wind energy introduces uncertainty into the grid due to its variable nature, thus increasing the chances of load curtailment. In this work, a probabilistic approach is used to determine the power and energy capacity of the ESS required to minimize this load curtailment. The goal of this approach is to determine the size of an ESS required to achieve a predetermined reliability target in a wind-integrated system.

A. Power Capacity

The power capacity of the ESS can be determined from the load curtailment of the system, which is affected by the variability of wind. The load curtailment at each time period can be obtained by modeling the components of the system as Markov chains and performing Monte Carlo simulation. Sequential simulation is used in this work to preserve the autocorrelation of the hourly wind speed model, which a non-sequential simulation might not be able to capture. The power system is represented by its components, which consist of conventional generators, wind turbine generators, transmission lines, and loads. Markov chains are used to model the components as two-state units, with the states being *up* and *down*. The MCS utilized to determine the load curtailment is implemented using the following steps [11].

1) Input failure rate and duration data for all components of the system.
2) Initialize all components in their *up* state.
3) Draw a random number for each component and calculate the time to the next event. The time to the next event for component i, T_i, is evaluated as follow.

$$T_i = -\frac{1}{\lambda_i}\ln(U_i) \tag{1}$$

   where U_i is a uniformly distributed random number and λ_i is the failure rate at the *up* state and the repair rate at the *down* state of the i^{th} component. Of these times, select the minimum time, $T_{\text{min}}(k)$. $T_{\text{min}}(k)$ denotes the time to the most imminent event, i.e., after $T_{\text{min}}(k)$, component k changes its state.
4) At each hour, check the component capacities and if they are adequate to satisfy the load then no curtailment occurs. However, load curtailment may be required in case of a contingency. In such a scenario, load curtailment is minimized by using an optimization framework and dispatch is rescheduled. More details pertaining to the optimization framework can be found be [11].
5) Reliability indices are accumulated, until a predetermined convergence criterion is met.

The process described above results in producing the entire probability distribution of hourly load curtailment in the system. Hence, the proposed approach offers the flexibility of sizing the ESS based on the risk the system operator is willing to undertake. In this work, the ESS is sized based on the mean value of load curtailment, which implies that the ESS will have a power capacity of P_L units if the mean hourly load curtailment is P_L units.

B. Energy Capacity

Let us assume that the availability of a wind-integrated system is A_0, and we need to increase its availability to A_1 using storage. Let us define a metric which we call unavailability reduction ratio, α, as follows.

$$\alpha = \frac{1 - A_1}{1 - A_0} \tag{2}$$

where $A_1 > A_0$. More details on how α is calculated for a wind-integrated system can be found in [12].

From section II-A, it is clear that the ESS needs to support a load of size P_L to increase system availability from A_0 to A_1 for a certain amount of time, which we assume to be t_A. The following relationship can be used to find a solution for t_A [7].

$$\int_{t_A}^{\infty} f_R(r)dr = \alpha \tag{3}$$

Equation (3) presents the basic expression that quantifies the ESS energy capacity required to improve the system availability from A_0 to A_1. However, in a practical world, ESS are not perfectly reliable, and that should be considered in the model. Let us assume that the ESS has an availability A_s. Then, the ESS must possess an energy capacity that allows it to supply a load P_L for time t_s, where t_s is expressed as follows.

$$t_s = \frac{t_A}{A_s} \tag{4}$$

Hence, the power capacity of the ESS should be at least P_L and its energy capacity should be at least $P_L t_s$ for improving the system availability from A_0 to A_1.

III. Sizing for Inertial Support

Frequency response plays a vital role in overall system dynamic performance. An imbalance in real power leads to frequency deviation from the nominal values and might result in load shedding. The swing equation, which dictates the behavior of system frequency in response to a change is load, can be expressed as follows [13].

$$\frac{2H}{f_s}\frac{df}{dt} = \frac{P_m - P_e}{S_{eq}} = \frac{\Delta P}{S_{eq}} \tag{5}$$

where H is the equivalent system inertia, f_s is the nominal frequency, $\frac{df}{dt}$ is the RoCoF, P_m and P_e are the mechanical power input and the electrical power output, and S_{eq} is the rated power of the system, respectively.

A. Maximum Frequency Deviation

A generalized load frequency control (LFC) model for a multi-machine system is utilized in this work [14] to determine the maximum allowable frequency deviation. This model has been shown to be fairly accurate for most applications, particularly at grid-scale where the dynamic contributions of inverters are not significant at today's renewable penetration

levels. The equation for frequency deviation can be developed from this LFC model [15] and is shown in (6). A summary of the notations used in equations (6)–(14) is given as follows.

H = equivalent inertia constant;
D = load damping constant;
K_i = LFC controller of machine i;
R_i = equivalent regulation constant of machine i
F_i = fraction of turbine power generated by high pressure (HP) unit of machine i;
T_i = governor time constant of machine i;
Δf = frequency deviation;
ΔP_L = disturbance;
m = total no. of machines in the system

$$\Delta f(s) = \frac{\frac{\Delta P_L}{s}}{D + 2Hs + \sum_{i=1}^{m} \frac{K_i(1+F_i T_R s)}{R_i(1+T_R s)}} \tag{6}$$

The governor time constants of all machines are assumed to be identical ($T_i = T_R,\ \forall\ i \in m$) , since the maximum frequency deviation has a low sensitivity to this quantity [14]. Applying inverse Laplace transformation, the expression for frequency deviation in the time domain is obtained as follows.

$$\Delta f(t) = \frac{\Delta P_L}{2HT_R\omega_n^2}\Bigg(1 - \frac{1}{\sqrt{1-\zeta^2}} e^{-\zeta\omega_n t}\cos\left(\omega_n\sqrt{1-\zeta^2}t - \phi\right)\Bigg) + \frac{\Delta P_L}{2H\omega_n\sqrt{1-\zeta^2}} e^{-\zeta\omega_n t}\sin\left(\omega_n\sqrt{1-\zeta^2}t\right)\Bigg) \tag{7}$$

where

$$F_R = \sum_{i=1}^{m} \frac{K_i F_i}{R_i} \tag{8}$$

$$R_R = \sum_{i=1}^{m} \frac{K_i}{R_i} \tag{9}$$

$$\omega_n = \sqrt{\frac{1}{2HT_R}(D + R_R)} \tag{10}$$

$$\zeta = \frac{1}{2}\frac{2H + T_R(D + F_R)}{\sqrt{2HT_R(D + R_R)}} \tag{11}$$

$$\phi = \tan^{-1}\left(\frac{\zeta}{\sqrt{1-\zeta^2}}\right) \tag{12}$$

The maximum frequency deviation is obtained by equating the derivative of $\Delta f(t)$ in (7) to zero and is expressed as follows.

$$\Delta f_{\text{max}} = \frac{\Delta P_L}{R_R + D}\left(1 + e^{-\zeta\omega_n t_{\text{max}}}\sqrt{\frac{T_R(R_R - F_R)}{2H}}\right) \tag{13}$$

where

$$t_{\text{max}} = \frac{1}{\omega_n\sqrt{1-\zeta^2}}\tan^{-1}\left(\frac{\omega_n\sqrt{1-\zeta^2}}{\zeta\omega_n - 1/T_R}\right) \tag{14}$$

B. Power Capacity of the ESS

Let the minimum inertia level required to maintain frequency within some pre-specified limits at time t be H_t^{min} for a particular disturbance event, and let the system equivalent inertia be H_t^{sys}. If $H_t^{\text{sys}} < H_t^{\text{min}}$, then an ESS may be deployed, which can inject active power into the system at a sufficiently high rate to maintain frequency stability. Hence, the inertia that the ESS needs to provide in such an event, can be defined as follows.

$$H_t^{\text{ESS}} = H_t^{\text{min}} - H_t^{\text{sys}} \tag{15}$$

Now, the relationship between H_t^{ESS}, and the real power injection required by the ESS for maintaining frequency stability, q_t^{int}, can be derived from (5) as follows [8].

$$H_t^{\text{ESS}} = q_t^{\text{int}}\frac{f_s}{2}\left(\frac{df}{dt}\right)^{-1} \tag{16}$$

This implies that the ESS should maintain a reserve of active power equal to q_t^{int} for time period t in order to satisfy the frequency stability constraint. The RoCof for this work has been assumed to be equal to 0.5 Hz/s [8].

The energy capacity of the ESS required for this application can be determined from the time period for which it needs to support the application. In general, inertial support is required for a few seconds before the primary frequency response of the system is activated. This time period is adjusted with t_s while calculating the total energy capacity of ESS and is further explained in section V-C.

IV. Modeling of Wind Power Output

This work focuses on improving the reliability of wind-rich systems and hence the modeling of wind power is an important aspect of the proposed framework.

A. Modeling of Wind Speed

Wind speed at a certain geographic location varies randomly with time. Hence, accurate models are needed to capture the various properties of wind speed. In this work, autoregressive moving average (ARMA) models are used to represent and forecast wind speed data. In statistical time series analysis, ARMA models can provide a description of a stationary stochastic process using observations from previous time steps. ARMA techniques have been widely used by researchers to model wind speed due to its accuracy [16]. An ARMA model is a combination of an autoregressive (AR) model and a moving average (MA) model. The AR model predicts the value of a variable using the observations of the previous time steps while the MA model uses the residuals of the previous forecasts. The number of previous observations used by the AR and MA models decide the parameters p and q of the ARMA model, respectively. In general, the value of a variable y at time t can be forecasted using an ARMA(p, q) model as follows.

$$\begin{aligned} y_t = \phi_1 y_{t-1} + \phi_2 y_{t-2} + ... + \phi_p y_{t-p} + \epsilon_t \\ + \theta_1\epsilon_{t-1} + \theta_2\epsilon_{t-2} + ... + \theta_q\epsilon_{t-q} \end{aligned} \tag{17}$$

where ϕ_i and θ_j are the parameters of the AR and MA models respectively; ϵ is an independently and identically distributed (IID) white noise process and $\epsilon \sim N(0, \sigma)$. The forecasted wind speed at time t, FW_t can then be obtained as a function of y_t.

$$FW_t = f(y_t) \tag{18}$$

The relationship between wind speed and wind power output is obtained from [17].

B. Wind Speed Data

Wind speed data for Albuquerque, NM, is collected from the National Renewable Energy Laboratory's (NREL's) Wind Prospector [18]. Three years of wind speed data, ranging from January 1, 2010, to December 31, 2012, is used to generate the ARMA model for this location. An AR model, a special case of an ARMA model, is used to model wind speed data at different locations. AR models are preferred for their simplicity and ease of interpretation and an AR model of appropriate order can be used to replace ARMA models without loss of accuracy [16]. The AR(8) model used to forecast wind speed data for Albuquerque is shown in (19). The accuracy of the AR model is- demonstrated by Figure 1, which shows the plots of the observed and the simulated wind speeds of Albuquerque.

$$\begin{aligned} y_t = {} & 0.7906y_{t-1} + 0.0.0318y_{t-2} - 0.0262y_{t-3} \\ & + 0.0003y_{t-4} - 0.0184y_{t-5} - 0.0174y_{t-6} \\ & - 0.0031y_{t-7} - 0.0082y_{t-8} + \epsilon_t \end{aligned} \tag{19}$$

where $\epsilon_t \sim N(0, 1.113)$.

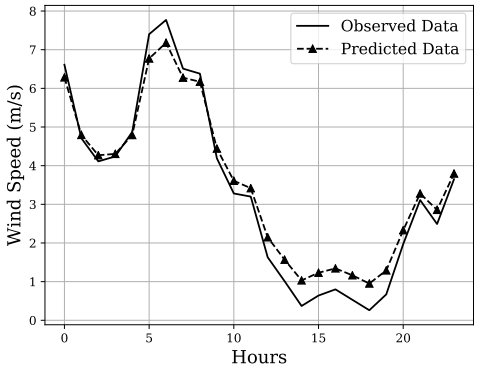

Fig. 1. Observed vs. predicted wind speed for Albuquerque for an example day.

V. Case Studies and Results

This section describes the test system and test cases, and discusses the results.

A. Test System

The efficacy of the proposed methodology is demonstrated using the Western System Coordinating Council (WSCC) 9-bus test system [19]. A single line diagram of the test system is shown in Fig. 2 and the generator data is provided in Table I. Two case studies are designed to test the efficacy of the proposed methodology as outlined in section V-B. In these case studies, the original system is modified by replacing part of the conventional generation with wind farms.

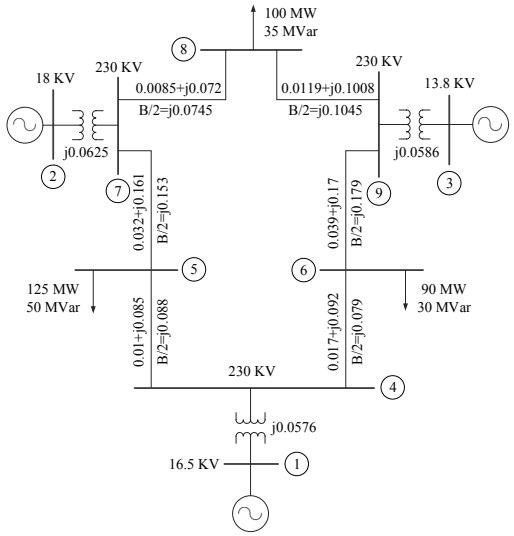

Fig. 2. Single line diagram of the WSCC 9-bus test system

TABLE I
Generator Data for the Test System

Gen. No.	Bus No.	Capacity (MW)	Inertia (s)
1	1	250	23.4
2	2	300	6.4
3	3	270	3.01

B. Case Studies

The following case studies are performed to evaluate the ESS size required to achieve a pre-determined reliability target and maintain frequency within some pre-specified limits in case of a disturbance. In each case, a load disturbance of 0.1 p.u. is considered. The inertia contribution from each turbine is assumed to be 0.025 s and the maximum frequency deviation is considered to be 0.015 Hz [4].

- **Case I:** Generator 3 of the test system is replaced by a wind farm of capacity 48 MW. This size is chosen as it makes up about 8% of the installed capacity in the system, the current share of wind power in the U.S. The wind farm is assumed to consist of 6 identical wind turbines of capacity 8 MW each.
- **Case II:** Generator 3 of the test system is replaced by a wind farm of capacity 144 MW. This size is chosen as it makes up about 20% of the installed capacity in the system, the target wind power share in the U.S by 2030 [20]. The wind farm is assumed to consist of 18 identical wind turbines of capacity 8 MW each.

TABLE II
ESS SIZES FOR THE CASE STUDIES

Case No.	$\bar{r}$ (h)	α	t_s (h)	P_L (MW)	$E[H_{\text{sys}}]$ (s)	H_{min} (s)	H_{ESS} (s)	P_{int} (MW)	P_{tot} (MW)
I	7.04	0.32	8	18.48	29.12	67.96	38.84	64.73	83.21
II	6.69	0.17	12	17.30	29.14	66.10	36.96	61.60	78.90

C. Results

Table II shows the results of the case studies. Here, P_L is calculated as the mean load curtailment of the system for a calendar day. P_{int}, which is calculated from q_t^{int}, denotes the storage quantity required for inertial support and P_{tot} denotes the total power capacity of the ESS required for serving both the applications. The energy capacity of the ESS is equal to $P_{\text{tot}} \times t_s$. The value of t_s has been rounded off to the nearest integer value greater than itself. This increment in the energy capacity of the ESS also ensures enough room for it to provide inertial support to the grid for a few seconds before primary frequency control is activated. Results show that the ESS size required in Case II is smaller than that in Case I, as the total generation of the system is greater in Case II, although serving the same load as in Case I.

VI. CONCLUSION

This paper proposed a new planning approach for mitigating the negative effects of integrating wind energy into the power grid using an ESS. In the proposed approach, the ESS is sized appropriately to provide inertial support and also minimize load curtailment of the system in the face of the low-inertia and variable characteristics of wind. A probabilistic method is developed for this purpose, which considers the failure of equipment leading to loss of load and low-inertia events in the system. An efficient MCS algorithm is used, which is capable of estimating the load curtailment and the inertia of the system in a single run, thus saving time and computational effort. A number of case studies are performed to demonstrate the ESS sizes required for maintaining frequency stability and achieving a predetermined reliability target under different wind penetration levels. The methodology developed and presented in this work can be utilized for planning of new ESS facilities or for more efficient utilization of existing ESS facilities integrated with wind generation.

ACKNOWLEDGMENT

The work presented in this paper was supported by the Energy Storage Program at the U.S. Department of Energy Office of Electricity. Sandia National Laboratories is a multi-mission laboratory managed and operated by National Technology and Engineering Solutions of Sandia, LLC., a wholly owned subsidiary of Honeywell International, Inc., for the U.S. Department of Energy National Nuclear Security Administration under contract DE-NA-0003525. This paper describes objective technical results and analysis. Any subjective views or opinions that might be expressed in the paper do not necessarily represent the views of the U.S. Department of Energy or the United States Government. The authors wish to thank Dr. Imre Gyuk for his continued support.

REFERENCES

[1] US Energy Information Administration (EIA), "The United States installed more wind turbine capacity in 2020 than in any other year," https://www.eia.gov/todayinenergy/detail.php?id=46976, accessed: 2021-11-03.

[2] International Renewable Energy Agency, "Future of Wind: Deployment, investment, technology, grid integration and socio-economic aspects," October 2019.

[3] N. Nguyen and J. Mitra, "An analysis of the effects and dependency of wind power penetration on system frequency regulation," *IEEE Trans. Sustain. Energy*, vol. 7, no. 1, pp. 354–363, 2015.

[4] N. Nguyen, A. Bera, and J. Mitra, "Energy storage to improve reliability of wind integrated systems under frequency security constraint," *IEEE Trans. Ind Appl.*, vol. 54, no. 5, pp. 4039–4047, 2018.

[5] A. Bera, S. Almasabi, Y. Tian, R. H. Byrne, B. Chalamala, T. A. Nguyen, and J. Mitra, "Maximising the investment returns of a grid-connected battery considering degradation cost," *IET Generation, Transmission & Distribution*, vol. 14, no. 21, pp. 4711–4718, 2020.

[6] P. Hu, R. Karki, and R. Billinton, "Reliability evaluation of generating systems containing wind power and energy storage," *IET Generation, Transmission & Distribution*, vol. 3, no. 8, pp. 783–791, 2009.

[7] J. Mitra, "Reliability-based sizing of backup storage," *IEEE Trans. Power Syst.*, vol. 25, no. 2, pp. 1198–1199, 2010.

[8] V. Knap, S. K. Chaudhary, D.-I. Stroe, M. Swierczynski, B.-I. Craciun, and R. Teodorescu, "Sizing of an energy storage system for grid inertial response and primary frequency reserve," *IEEE Trans. Power Syst.*, vol. 31, no. 5, pp. 3447–3456, 2015.

[9] H. Golpîra, A. Atarodi, S. Amini, A. R. Messina, B. Francois, and H. Bevrani, "Optimal energy storage system-based virtual inertia placement: A frequency stability point of view," *IEEE Trans. Power Syst.*, vol. 35, no. 6, pp. 4824–4835, 2020.

[10] A. Bera, M. Abdelmalak, S. Alzahrani, M. Benidris, and J. Mitra, "Sizing of energy storage systems for grid inertial response," in *2020 IEEE Power and Energy Society General Meeting*, Aug. 2020, pp. 1–5.

[11] C. Singh, P. Jirutitijaroen, and J. Mitra, *Electric Power Grid Reliability Evaluation: Models and Methods*. Wiley-IEEE Press, 2018.

[12] S. Sulaeman, Y. Tian, M. Benidris, and J. Mitra, "Quantification of storage necessary to firm up wind generation," *IEEE Trans. Ind. Appl.*, vol. 53, no. 4, pp. 3228–3236, 2017.

[13] V. Vittal, J. D. McCalley, P. M. Anderson, and A. Fouad, *Power System Control and Stability*. John Wiley & Sons, 2019.

[14] H. Ahmadi and H. Ghasemi, "Security-constrained unit commitment with linearized system frequency limit constraints," *IEEE Trans. Power Syst.*, vol. 29, no. 4, pp. 1536–1545, 2014.

[15] N. Nguyen, S. Almasabi, A. Bera, and J. Mitra, "Optimal power flow incorporating frequency security constraint," *IEEE Trans. Ind. Appl.*, vol. 55, no. 6, pp. 6508–6516, 2019.

[16] R. Billinton, H. Chen, and R. Ghajar, "Time-series models for reliability evaluation of power systems including wind energy," *Microelectronics Reliability*, vol. 36, no. 9, pp. 1253–1261, 1996.

[17] R. Billinton and G. Bai, "Generating capacity adequacy associated with wind energy," *IEEE Trans. Energy Convers.*, vol. 19, no. 3, pp. 641–646, 2004.

[18] "The Wind Prospector," https://maps.nrel.gov/wind-prospector/, accessed: 2021-03-23.

[19] P. W. Sauer and M. A. Pai, *Power System Dynamics and Stability*. Prentice Hall Upper Saddle River, NJ, 1998, vol. 101.

[20] US Department of Energy, "20% wind energy by 2030: Increasing wind energy's contribution to US electricity supply," *Energy Efficiency and Renewable Energy Tech. Rep. DOE/GO*, pp. 102 008–2567, 2008.